A self-calibrating wide range electrometer for in-cloud measurements

Harrison, G. ORCID: https://orcid.org/0000-0003-0693-347X, Nicoll, K. ORCID: https://orcid.org/0000-0001-5580-6325, Marlton, G., Williams, P. ORCID: https://orcid.org/0000-0002-9713-9820 and Airey, M. ORCID: https://orcid.org/0000-0002-9784-0043 (2017) A self-calibrating wide range electrometer for in-cloud measurements. Review of Scientific Instruments, 88 (12). 126109. ISSN 0034-6748 doi: 10.1063/1.5011177 Available at https://centaur.reading.ac.uk/74379/

Note: A self-calibrating wide range electrometer for in-cloud measurements

R. Giles Harrison, Graeme J. Marlton, Keri A. Nicoll, Martin W. Airey, and Paul D. Williams

Citation: Review of Scientific Instruments **88**, 126109 (2017); doi: 10.1063/1.5011177
View online: https://doi.org/10.1063/1.5011177
View Table of Contents: http://aip.scitation.org/toc/rsi/88/12
Published by the American Institute of Physics

Note: A self-calibrating wide range electrometer for in-cloud measurements

R. Giles Harrison,[1] Graeme J. Marlton,[1] Keri A. Nicoll,[1,2] Martin W. Airey,[1] and Paul D. Williams[1]
[1]*Department of Meteorology, University of Reading, Earley Gate, Reading RG6 6BB, United Kingdom*
[2]*Department of Electronic and Electrical Engineering, University of Bath, Bath BA2 7AY, United Kingdom*

(Received 30 October 2017; accepted 4 December 2017; published online 18 December 2017)

Charge is observed in clouds of all forms, which may influence their development and properties. In-cloud charge measurements require a wide dynamic range, extending from charge in aerosols and dusts to that present in thunderstorms. Unexpectedly large charge densities (>200 pC m^{-3}) have recently been detected in layer clouds using balloon-carried linear electrometers. These, however, lead to instrument saturation if sufficient sensitivity for aerosol and droplet charge is maintained. Logarithmic electrometers provide an alternative but suffer strong non-linear thermal effects. This is a limitation for balloon-carried instruments that encounter temperature changes up to ~100 °C, as full thermal compensation requires complexity inappropriate for disposable devices. Here, a novel hybrid system is described, combining linear and logarithmic electrometers to provide extended dynamic range (±50 pA), employing the negligible (±4%) total temperature drift of the linear device to provide *in situ* calibration of the logarithmic device. This combination opens up new measurement opportunities for charge in clouds, dusts, and aerosols. https://doi.org/10.1063/1.5011177

Enhancing the standard use of *in situ* measurement platforms, such as meteorological balloons already used for cosmic rays,[1] energetic particles,[2] cloud backscatter,[3] turbulence,[4] and charge,[5] provides a flexible method for data collection at heights extending from the surface to 30 km. Obtaining charge measurements within clouds, however, can present difficulties if the charge encountered is large, as is often the case during disturbed weather, or when the cloud contains both ice and liquid water. Some extreme charge densities (>200 pC m^{-3}) have even been observed in layer clouds,[5] but they have yet to be quantified. Whilst our existing charge sensor[6] is sufficiently sensitive to detect the charge associated with aerosol[7] and dust[8] layers, extending its use to more highly charged cloud situations would require reduction in its gain, with an associated lessened sensitivity. A possible alternative is to use a logarithmic response; light-tight light-emitting diodes (LEDs) provide this characteristic, previously used in an electrometer operating over many orders of magnitude of current.[9]

The logarithmic approach has already been employed effectively to measure the point discharge current in the atmosphere, which spans at least six orders of magnitude in current (pA–μA) between fair weather and thunderstorm conditions.[10] A difficulty with such logarithmic electrometers, however, is their substantial temperature dependence. This would be particularly troublesome for balloon-carried sensors, where the temperatures encountered in an hour-long ascent change rapidly, typically from 20 °C to −60 °C. Thermally compensated logarithmic electrometers are useful for more slowly changing surface atmospheric temperatures,[10] but even implementing this requires the inclusion of symmetrical circuit elements having a matched thermal response, as well as ensuring temperature tracking in other components accurately follows that in the logarithmic elements.[9] Adopting the same approach for a balloon-carried instrument would add cost and complexity to a device which is generally regarded as disposable. There are two further disadvantages. First, whilst a logarithmic device does extend the dynamic range effectively, it also brings a loss of resolution and sensitivity when compared with a linear device. Second, at small currents (<1 pA), the time response becomes considerable (>10 s), which, coupled with the ascent speed of the balloon, could lead to important atmospheric features being missed. Although the time response can be improved, further circuitry is again required.[11]

To minimize the complexity whilst providing a wide dynamic range of measuring currents, a hybrid device combining linear and logarithmic response from two separate sensing electrodes has been developed. This maintains the good sensitivity of the linear devices but provides the additional dynamic range possible from a logarithmic device.

The instrument consists of two identical hollow spherical electrodes (diameter 12 mm), mounted on opposite sides of a 3d-printed box (700 mm × 700 mm × 400 mm). These sense induced atmospheric currents[6] as the balloon-carried system ascends. They are connected to two separate electrometers, each using a low bias current operational amplifier. The output voltages derived are sent over the UHF telemetry of a standard meteorological radiosonde, using the PANDORA connection system.[12]

Figure 1 shows the principal electronic aspects of the measurements. The sensing electrodes provide current at S1 and S2 for the linear current amplifier stage (constructed around U1), and logarithmic stage (using U2), respectively, via

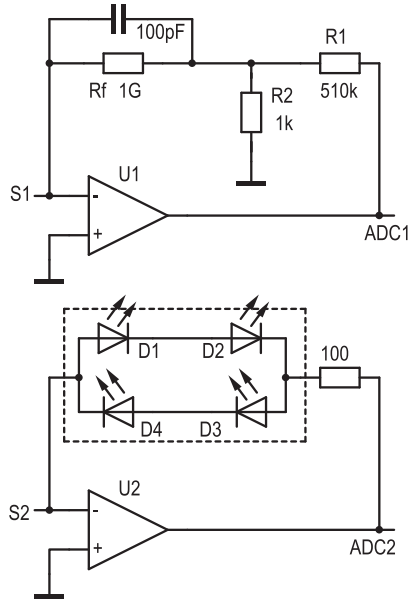

FIG. 1. Outline schematic of the input stages of the hybrid measurement system. Identical sensing electrodes S1 and S2 are connected to U1 and U2, wired as (bipolar) linear and logarithmic current amplifiers, respectively. The logarithmic stage uses light-tight green light-emitting diodes as feedback elements. Output voltages are presented to analog to digital converter stages at ADC1 and ADC2.

air-wired and PTFE-insulated connections. The linear stage uses a feedback resistance synthesized from a T-network of resistors (R_f, R1, R2). Its effective feedback resistance R_{eff} is

$$R_{eff} = R_f\left[1 + \frac{R1}{R2}\right], \tag{1}$$

which, for the component values chosen, has R_{eff} = 510 GΩ. The output voltage V_1 for an input current i_1 from S1 is

$$V_1 = -i_1 R_{eff}, \tag{2}$$

or about ±5 pA for a 5 V input range. The input current i_2 from the second sensor S2 is taken to a logarithmic current amplifier, employing two series-connected green LEDs as the feedback elements and wired in inverse parallel with a second pair of LEDs to allow measurement of bipolar currents. (Each of the four LEDs was coated with black nail varnish before assembly.) The output voltage V_2 is given by[9]

$$V_2 = -2\frac{kT}{e}\ln\left(\frac{i_2}{I_0}\right), \tag{3}$$

where

$$I_0 = kT^3\exp\left(\frac{-E_b}{kT}\right). \tag{4}$$

In these equations, e is the elementary charge, k is Boltzmann's constant, T is the temperature, I_0 is the reverse saturation current, and E_b is the bandgap of the semiconductor used in the LED.

Equations (3) and (4) show there is temperature dependence in the logarithmic system, for which, as mentioned, full compensation of the different terms is complex. In contrast, Eqs. (1) and (2) describing the linear system show no fundamental temperature sensitivity. The temperature response of the linear electrometer instead arises from component effects, principally the thermal response of the resistors in the T-network and R_f in particular. The particular component used for R_f, a thick-film 0.25 W resistor (Neohm RGP0207CHK1G0) has a specified tolerance of ±10% and a temperature coefficient of ±350 ppm °C^{-1}; R1 and R2 are thin film 0.125 W ± 1%, ±50 ppm °C^{-1} components. Combined effects of R1, R2, and R_f lead to a current measurement error <±4% over the typical maximum temperature change of 100 °C, as previously verified experimentally.[6]

Rather than adding complexity to achieve temperature compensation of the logarithmic electrometer, the principle adopted here is to expose the two separate sensors to the same atmospheric circumstances and use the much better relative temperature stability of the linear stage to provide *in situ* calibration of the logarithmic stage.

This approach has been tested in flight, carrying the two electrometers on a Vaisala RS92 radiosonde with a PANDORA interface system. The electrodes were mounted securely on opposite sides of the box housing the PANDORA interface, with the electrode connection wire perpendicular to the box, also providing mechanical support. Figure 2 shows measurements through a low level drizzling layer cloud, with the meteorological data. The vertical stripes of points left and right on Fig. 2(a) indicate positive and negative saturation in the linear device, which does not occur with the logarithmic device [Fig. 2(b)].

Calibration of the logarithmic electrometer S2 is obtained by matching its output to calibrated currents from the linear sensor S1, using in-flight values to ensure that no further

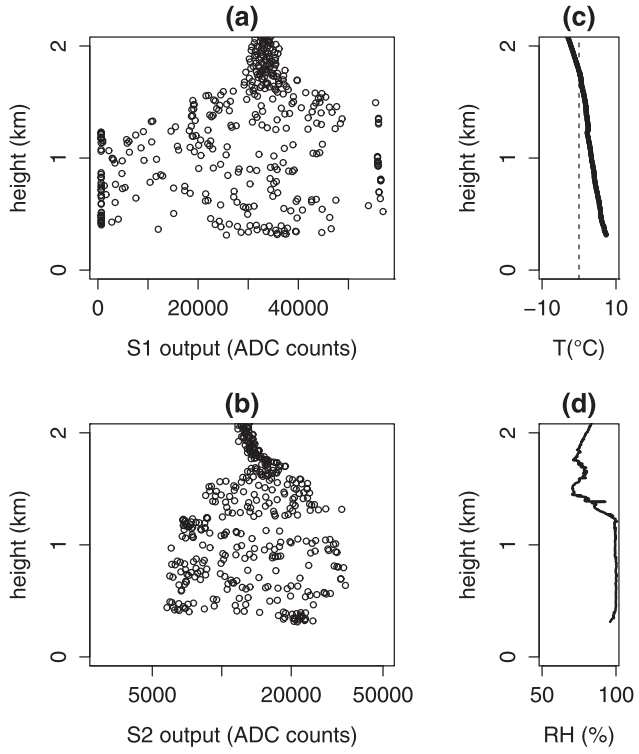

FIG. 2. Measurement (1 s intervals) using (a) linear and (b) logarithmic electrometers ascending through a drizzle-generating cloud. Results are in Analog to Digital Converter (ADC) counts, where values from 0 to 65 535 represent the bipolar output voltage. (c) and (d) show the air temperature (T) and Relative Humidity (RH), respectively.

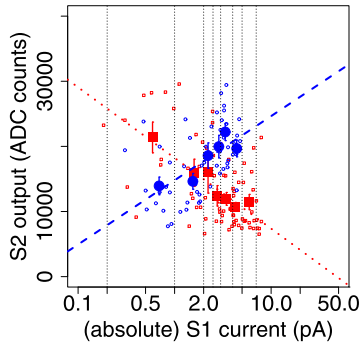

FIG. 3. Calibrated linear electrometer output (S1) against logarithmic electrometer output (S2), for in-flight values. Small circles and squares denote negative and positive currents, respectively, as determined by the linear electrometer. Larger symbols show binned values, with one standard error. Dashed and dotted lines show least squares fits for negative and positive currents, respectively, weighted by the inverse standard errors.

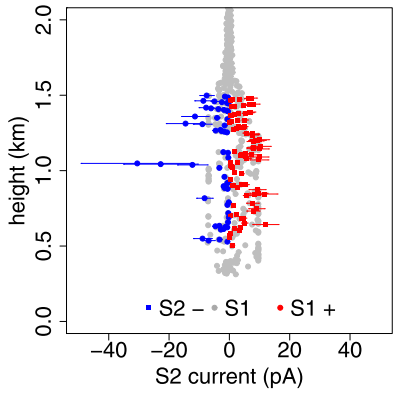

FIG. 4. Calibrated logarithmic sensor currents S2, for positive (red squares) and negative (blue dots) currents, as determined by the linear sensor. Grey points show the currents found by the linear sensor, S1. (Error bars show the equivalent range of one standard error, from multiple realisations of the fits in Fig. 3).

temperature correction is needed. The S1 measurement values were first converted to current using Eqs. (1) and (2), with the known values of Rf, R1 and R2.

Figure 3 shows calibrated currents from the linear sensor, plotted against the output of the logarithmic sensor. The individual points show some scatter, as the sensors do not encounter exactly the same environment because of package swing, and the time response becomes appreciable for the logarithmic sensor at small currents. The values sampled are also uneven across the measurement range. Binning has been used to provide approximately equal numbers of samples. This clearly shows the logarithmic response, in principle measureable to beyond ±50 pA.

As different feedback components are used in the logarithmic electrometer for the two polarities, the fitting coefficients also differ. It is necessary to choose the positive or negative fitting coefficients, using the linear electrometer as a polarity selector.

The weighted fit lines shown in Fig. 3 provide calibration coefficients for the data of the form

$$S_2 = m_\pm \log i_1 + c_\pm, \tag{5}$$

allowing the current i_2 flowing from S2 to be determined from the recorded ADC values as

$$i_2 = 10^{\left(\frac{S2-c_\pm}{m_\pm}\right)}. \tag{6}$$

Figure 4 shows the effect of applying the calibrations from Fig. 3 to the S2 data in Fig. 2, compared with the calibrated values from the linear sensor S1. The range of the logarithmic sensor is greater than that of the linear sensor, with similar cloud charge structures measured by both sensors, such as at 1.2 km.

Combining linear and logarithmic electrometers provides a disposable self-calibrating system without the complexity of full temperature compensation, allowing the detailed structure of more strongly electrified clouds to be explored.

The radiosonde measurement packages were funded by the UK Natural Environmental Research Council (Grant No. NE/P003362/1), with support for KAN from No. NE/2011514/1. We thank David Brus for logistics during the Pallas Cloud Experiment 2017, supported by the EU ACTRIS-2 fund for Transnational Access.

[1]R. G. Harrison, K. A. Nicoll, and K. L. Aplin, J. Atmos. Sol.-Terr. Phys. **119**, 203–210 (2014).
[2]K. L. Aplin, A. A. Briggs, R. G. Harrison, and G. J. Marlton, Space Weather **15**, 663, https://doi.org/10.1002/2017SW001610 (2017).
[3]R. G. Harrison and K. A. Nicoll, Rev. Sci. Instrum. **85**, 066104 (2014).
[4]G. J. Marlton, R. G. Harrison, K. A. Nicoll, and P. D. Williams, Rev. Sci. Instrum. **86**, 016109 (2015).
[5]K. A. Nicoll and R. G. Harrison, Q. J. R. Meteorol. Soc. **142**, 2679–2691 (2016).
[6]K. A. Nicoll, Rev. Sci. Instrum. **84**, 096107 (2013).
[7]R. G. Harrison, K. A. Nicoll, Z. Ulanowski, and T. A. Mather, Environ. Res. Lett. **5**, 024004 (2010).
[8]K. A. Nicoll, R. G. Harrison, and Z. Ulanowski, Environ. Res. Lett. **6**(1), 014001 (2011).
[9]Y. B. Acharya and S. G. Tikekar, Rev. Sci. Instrum. **64**(6), 1652–1654 (1993).
[10]G. J. Marlton, R. G. Harrison, and K. A. Nicoll, Rev. Sci. Instrum. **84**, 066103 (2013).
[11]Y. B. Acharya and P. D. Vyavahare, Int. J. Electron. **86**(8), 999–1011 (1999).
[12]R. G. Harrison, K. A. Nicoll, and A. G. Lomas, Rev. Sci. Instrum. **83**(3), 036106 (2012).